Driving voltage reduction in white organic light-emitting devices from selectively doping in ambipolar blue-emitting layer

Chih-Hung Hsiao, Chi-Feng Lin, and Jiun-Haw Lee
Graduate Institute of Photonics and Optoelectronics and Department of Electrical Engineering, National Taiwan University, No. 1, Sec. 4, Roosevelt Road, Taipei, Taiwan

(Received 30 July 2007; accepted 13 September 2007; published online 7 November 2007)

White organic light-emitting devices (OLEDs) consisting of ambipolar 9,10-bis(2′-naphthyl) anthracene (ADN) as a host of blue-emitting layer (EML) were investigated. A thin codoped layer of yellow 5,6,11,12-Tetraphenylnaphthacene (rubrene) served as a probe for detecting the position of maximum recombination rate in the 4,4′-bis[2-(4-(*N*,*N*-diphenylamino)phenyl)vinyl] biphenyl (DPAVBi) doped-ADN EML. Due to the energy barrier and bipolar carrier transport, the maximum recombination rate was found to be close to but not exactly at the interface of the hole-transporting layer and the EML. With appropriate tuning in the thickness, position, and dopant concentrations of the codoped layer (rubrene:DPAVBi:ADN) in the EML, the device driving voltage decreased by 21.7%, nearly 2 V in reduction, due to the increased recombination current from the faster exciton relaxation induced by the yellow dopants. Among the advantages of introducing the codoped layer over conventional single-doped layers are the elimination of the trapping effect to avoid increasing the device driving voltage, the alleviation of the dependence of the recombination zone on the applied voltage for improving color stability, and the utilization of excitons in a more efficient way to enhance device efficiency. Without using any electrically conductive layers such as the *p-i-n* structure, we were able to successfully generate 112 cd/m^2 at 4 V from our white OLED simply by engineering the structure of the EML. © *2007 American Institute of Physics*.
[DOI: 10.1063/1.2804757]

I. INTRODUCTION

Since stacked organic thin solid films emit light with practical applied voltage of less than 10 V, organic light-emitting devices (OLEDs) have been touted as a promising display technology for the next generation.[1] By virtue of easy fabrication, self-emission, color saturation, and flexibility, OLEDs have triggered a new wave of research into device structure and material promotion. Initially, most of the research efforts were targeted at monochromatic OLEDs, in attempts to raise the efficiency and operation lifetime. After much of the underlying physics was understood, white OLEDs, which can act as surface light sources, have emerged as candidates for backlight application as well as solid-state lighting in the future.[2]

A conventional way to create white OLEDs is by stacking emitting layers (EMLs) of different colors together.[3–5] However, under the requirement of simple device structures, single nondoped EMLs have been developed to generate white light by means of exciplex emission.[6,7] A similar method utilizes a stack of devices, also known as a tandem device. The tandem structure not only stacks the efficiency of each device, but also further increases the total device efficiency due to the microcavity effect.[8] A concept borrowed from semiconductor LED led to the development of phosphor-coating blue OLEDs. A maximum efficiency of as high as ~40 cd/A at 500 cd/m^2 had been achieved by this down-conversion method. However, this is not a wholly organic device. A more advanced design on device configuration is the exciton harvesting structure, which enables good management on the singlet and triplet excitons.[9] Forcing singlet excitons to the fluorescent blue dopants, and triplet excitons to the phosphorescent red and green dopants is the key idea in accomplishing nearly 100% internal quantum efficiency. In the context of device efficiency, the exciton harvesting structure manages 23.8 lm/W at 500 cd/m^2. In terms of emitting materials, phosphorescent materials represent a grand new approach for enhancing device efficiency. They efficiently utilize triplet excitons, which are usually wasted in fluorescent materials.[10] In particular systems, they serve as phosphorescent sensitizer to trigger originally inhibited energy transfer from the triplet state of the sensitizer to the singlet state of the fluorescent dye.[11] Although these applications of phosphorescent materials can realize nearly 100% internal quantum efficiency, there are two pressing issues to be addressed: typical efficiency roll-off at high current injection due to triplet-triplet annihilation,[12] and the lack of blue phosphorescent materials available commercially.[13] Therefore, we focus on the fluorescent materials to circumvent these pitfalls, and propose a new architecture to enhance efficiency without the need for higher efficiency phosphorescent materials.

One of the major drawbacks of white OLEDs is the color-shifting phenomenon induced mainly by the recombination rate (*R*-rate) distribution shift under various applied voltages or during device aging.[2,14] The *R*-rate often has a maximum value at certain interface in the heterojunction device and decreases rapidly away from the interface, thus leading to a narrow recombination zone around the interface.[15] Compared with heterojunction device, ambipolar materials such as mixed-host and 9,10-bis(2′-naphthyl) an-

thracene (ADN), which eliminate the abrupt barrier at the interface, give rise to a broad recombination zone (R-zone) in the EML. It is believed that a wider R-zone will release some vital stress during the device operation, thereby improving the device lifetime.[16–18]

Our recent study showed that the appropriate incorporation of an ultrathin doped layer in the ambipolar EML can effectively reduce driving voltage by ~20%.[19] In this case, the voltage reduction is exactly the manifestation of current enhancement caused by increasing opposite carriers' recombination. Under the steady state, the recombination current (J_r) can be deduced from the continuity equation,

$$J_r = \int_0^L eRdx, \tag{1}$$

$$R = \gamma np, \tag{2}$$

where e is one electron charge, L is the length of EML, R is the recombination rate, γ is the recombination coefficient, and $n(p)$ is electron (hole) concentration. In our prior experiment,[19] 4-(dicyanomethylene)-2-tert-butyl-6–1,1,7,7-tetramethyljulolidyl-9-enyl)-4H-pyran (DCJTB) was used as a dopant in an ambipolar host, actually a mixed host, of 50% N,N'-diphenyl-N,N' -bis(1-napthyl)-1,1′-biphenyl-4,4′-diamine (NPB) and 50% tris-(8-hydroxyquinoline) aluminum (Alq3). Red, green, and yellow colors were observed from the red-emitting dopant, the green-emitting mixed-host, and their combination. With proper tuning of the DCJTB position, the obvious driving voltage reduction occurred only when the DCJTB molecules appeared around the position of maximum R-rate.

In this study, blue ambipolar ADN (Refs. 17 and 20) and complementary yellow fluorescent dopant, 5,6,11,12-tetraphenylnaphthacene (rubrene), were used to obtain white OLEDs. Molecule structures of all the organic materials are shown in Fig. 1(a). A greenish-blue fluorescent dopant, 4,4′-bis[2-(4-(*N*,*N*-diphenylamino)phenyl)vinyl]biphenyl (DPAVBi) was entirely doped in the EML, while the yellow fluorescent rubrene was partially doped in certain position to provide the same function as the DCJTB in Ref. 19. Combining complementary emission from two different dopants and voltage reduction from rubrene, white light with low driving voltage was achieved. Although the organic materials in this study are common and commercially available, our white OLED exhibited superior device performances to those with conventional heterojunction[21] and totally doped EML.[22] Unlike the *p-i-n* structure,[23] which reduces the driving voltage by improving the injection and transport capability, only the EML structure was engineered in this study. In terms of device performances, our white OLED managed 112 cd/m^2 at 4 V, comparable to *p-i-n* devices with 100 cd/m^2 at ~3 V.

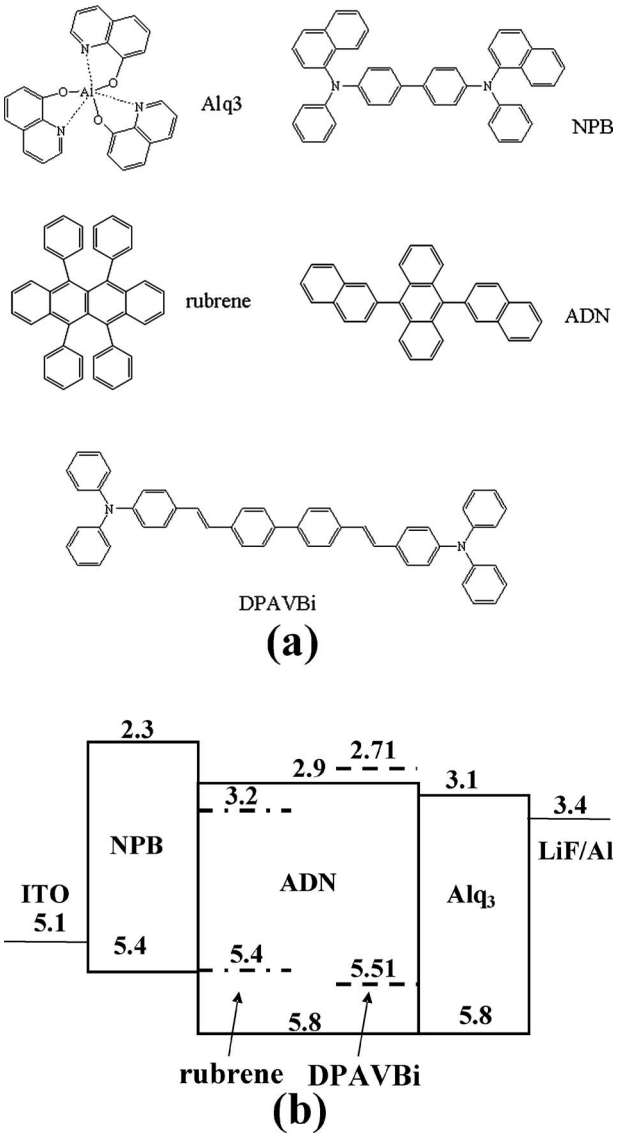

FIG. 1. (a) Molecule structures of NPB, ADN, Alq3, rubrene, and DPAVBi. (b) HOMO and LUMO level of all used organic materials, ITO, and LiF/Al.

II. EXPERIMENTS

Indium-tin-oxide (ITO) glass with low sheet resistance of 10 ohm/sqr and surface roughness of less than 1 nm was used as the substrate. The active region size of the test pixel is 2×2 mm. Before deposition of organic materials, the standard precleaned process of ITO-coated glass was performed, followed by treatment with oxygen plasma to increase its work function. The substrate was then loaded in a high vacuum chamber (~3×10^{-6} Torr) to grow the desired organic materials by thermal evaporation. Finally, the as-fabricated device was hermetically sealed by UV-cured epoxy in a nitrogen glove box. The current-density-voltage ($J-V$) characteristics were measured by means of a Keithley 2400 source meter. The electroluminescence spectra were obtained with a Minolta CS-1000 spectrometer.

The backbone, blue EML, of the white OLED is DPAVBi-doped ADN 45 nm in thickness. The EML was sandwiched by a 40 nm hole-transporting layer (HTL) of NPB on the anode side and a 15 nm electron-transporting layer (ETL) of Alq3 on the cathode side. A conventional cathode, LiF/Al, was formed in successive step. During the fabrication of the white OLEDs, the yellow-emitting rubrene was codoped into the blue EML. Figure 1(b) illustrates the

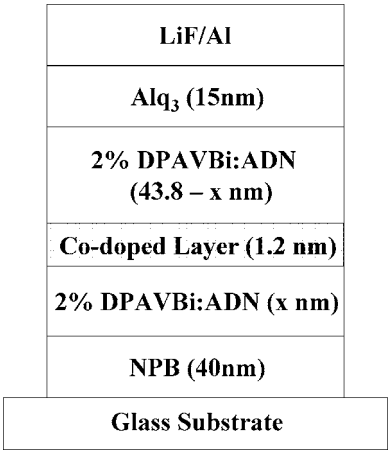

FIG. 2. Device configurations of device 2–4. The codoped layer with 1.2 nm in thickness consists of 2% rubrene and 2% DPAVBi. Device 1 is the reference device without rubrene, that is, no codoped layer. The parameter x denotes the distance from the NPB interface to the codoped layer. Devices with x=0, 5, 10 are labeled as device 2, 3, 4, respectively.

highest occupied molecular orbital (HOMO) and the lowest unoccupied molecular orbital (LUMO) values of all materials used in the devices.

III. RESULTS AND DISCUSSION

A. *R*-rate distribution in 2% DPAVBi-doped EML

To investigate the *R*-rate distribution in the EML of 2% DPAVBi:ADN, an ultrathin (1.2 nm) codoped layer consisting of 2% rubrene:2%DPAVBi:ADN was used as a probe, as illustrated in Fig. 2. Since the rubrene has a higher recombination coefficient than the DPAVBi, the probe played the same role as that in Ref. 19 in retrieving the information on the driving voltage at fixed current density with respect to the probe position, thereby yielding the *R*-zone profile in the EML.

Figure 3 shows that device 3 had the lowest driving voltage of 7.85 V at 100 mA/cm^2, while the $J-V$ characteristics for the other devices were nearly identical, around 9.16 V at the same injection level. The voltage reduction of 14.3% in device 3 indicated that the probe position coincided with the position of maximum *R*-rate, 5 nm away from HTL/EML interface. The fact that the hole-injection barrier from the

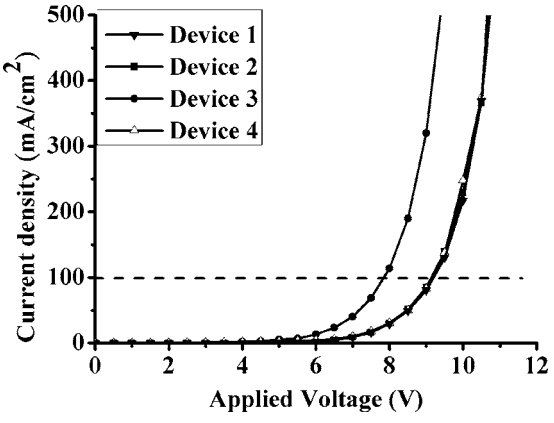

FIG. 3. $J-V$ characteristics of device 1–4.

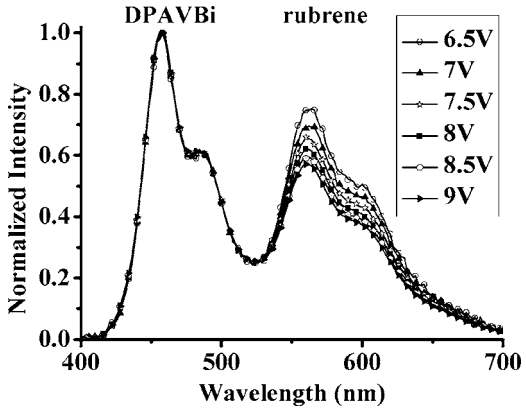

FIG. 4. Emission spectra of device 3.

HTL to the EML was larger than its electron-injection counterpart from the ETL to the EML accounted for the deviation of the maximum *R*-rate from the interface.

Figure 4 traces the spectra evolution of device 3 under different driving voltages. As the applied voltage was increased, the emission from the DPAVBi grew, since there were insufficient yellow-emitting rubrene sites (2% in 1.2 nm) to accommodate the increasing number of excitons formed by the injected carriers. The shifting locus of the Commission Internationale d'Eclairage (CIE) coordinates almost passed through the pure white light point (0.33, 0.33). This phenomenon implied that dedicated control of probe conditions such as doped concentration, thickness, and position cannot only generate white light, but can also reap the advantage of voltage reduction.

B. Device structure simplification

To realize the above-mentioned white OLED and to keep the device simple, we replaced the ultrathin probe with a thin codoped layer, as shown in Fig. 5. In devices 5–7, the rubrene concentration of the fixed 5 nm thick codoped layer was an adjustable parameter. The 5 nm thick layer was used to at least cover the maximum *R*-rate position. Device 5–7 contained 2%, 3%, 4% rubrene in codoped layer, respectively.

According to the $J-V$ characteristics listed in Table I, higher rubrene concentration retards carrier transport through the thin codoped layer, thus increasing the driving voltage. This trend accounts for the carrier trapping effect, which is conventionally believed to be more significant in the case of higher dopant concentration. Device 5 with 2% rubrene exhibited the lowest driving voltage due to the fact that there was the least perturbation in carrier transport. From Table I, device 6 with a slightly higher driving voltage exhibited the highest luminance and power efficiencies of 6.34 cd/A and 3.64 lm/W at 5.5 V corresponding to 200 cd/m^2. Device 6 sacrificed driving voltage in exchange for higher efficiency, as more trapping sites of rubrene were introduced to facilitate a more efficient energy transfer. Reduction in the efficiency accompanying the blueshift effect under increasing applied voltage indicated that more excitons will be released radiatively through the less efficient DPAVBi due to the saturation of the rubrene molecules. This explanation is sup-

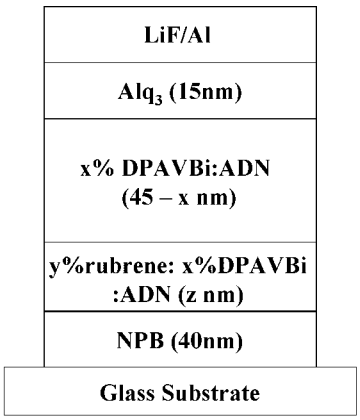

(a)

Device	x% DPAVBi	y% rubrene	Codoped layer z nm
5	2	2	5
6	2	3	5
7	2	4	5
8	3	ref. device without codoped layer	
9	3	3	5
10	3	3	10
11	3	3	15
12	0	2	5

(b)

FIG. 5. (a) Device configurations of device 5–12. The parameters *x*, *y*, and *z* denote the dopant concentration of DPAVBi and rubrene, and the thickness of codoped layer, respectively. (b) The parameters of device 5–12. Device 12 is similar to device 5 except for the absence of DPAVBi in the codoped layer.

ported by the fact that the efficiency of the white OLED approached that of the reference blue OLED at higher voltages.

C. Device fine-tune and optimization

The concentration of 3% DPAVBi is the optimal value over the range from 2% to 4%.[13] The $J-V$ characteristic of the 3% DPAVBi-doped control device 8 (the same device architecture as device 1) was almost identical to that of device 1, except for a slightly lower driving voltage and a higher current efficiency. Although the HOMO difference between the DPAVBi and the ADN is 0.3 eV, the hole-transporting property of the DPAVBi enables holes to hop through them, partially compensating for the negative influence of the energy barrier on carrier transport. In that regard, increasing the DPAVBi concentration reduces the driving voltage.[13]

TABLE I. Device performance in terms of the driving voltage, maximum luminance, and power efficiency.

Device	Driving voltage (V) @ 100 mA/cm^2	Max. luminance efficiency (cd/A)	Max. power efficiency (lm/W)
1	9.17	4.4	1.8
5	8.08	5	2.9
6	8.58	6.34	3.64
7	8.88	6.17	3.25
8	9.12	5.9	2.85
9	8.75	5.75	3
10	7.16	7.7	6.2
11	8.47	6.5	4.8
12	9.75	4.4	2.25

Similar device architectures discussed in Sec. III A were used to investigate the effect under different DPAVBi concentrations. Referring to Fig. 5, devices 9–11 were fabricated with codoped layers of varying thicknesses. The $J-V$ characteristics of devices 9–11 are shown in Table I. Device 10 exhibited the lowest driving voltage, which dropped by as much as 2 V relative to device 8. It is noticeable that the thickness of the codoped layer in device 10 was twice that in device 6. According to the discussion in previous sections, the position of maximum *R*-rate was 10 nm away from NPB layer in the case of 3% DPAVBi doped devices. This is a corollary of the effect of the higher concentration of hole-transporting DPAVBi in device 10. The presence of more DPAVBi enabled more holes to penetrate deeper into EML, resulting in the deviation of the maximum *R*-rate position further from the NPB/EML interface.

The thickness of the codoped layer plays an important role in the $J-V$ characteristic. The $J-V$ curves of device 9 and 11 with 5 and 15 nm rubrene-codoped layer, respectively, were close to, but somewhat lower than, device 8. Before elucidating the dependence of the current behavior on the thickness, the *R*-rate distribution in 2% and 3% DPAVBi-doped EML should be discussed. Returning to Fig. 3, which depicted the relation between the current density and the rubrene probe position, it was found that the voltage reduction phenomenon disappeared as long as the probe was not lying in the maximum *R*-rate position. Excluding the carrier-trapping effect of the rubrene probe, the above observation revealed that the *R*-rate dropped sharply from its maximum value. On the other hand, in the 2% DPAVBi-doped devices, the recombination distribution was centered at 5 nm to the NPB/EML interface, with the FWHM of *R*-zone being narrower than 10 nm. Coming back to device 9, one can see that even if the codoped layer was located 5 nm away from maximum *R*-rate position, a slight voltage reduction was still observed. This result indicated that the *R*-rate distribution centered at 10 nm was broader than that in the 2% DPAVBi devices. It is reasonable to surmise that *R*-distribution was widened due to the more energetic and structural disorder introduced by the presence of more DPAVBi molecules.[24,25] Device 11 also had a similar $J-V$ curve as device 9, but the underlying mechanism was different. In device 9, the voltage reduction came from the slightly enhanced recombination current, whereas in device 11, the voltage reduction resulted from the complex combination of the enhanced recombination current and the increased electron trapping effect from rubrene. In device 11, the first 10 nm, near the NPB side, of the 15 nm codoped layer enhanced the recombination current since it covered the maximum *R*-rate position. However, the remaining 5 nm, which was in between the maximum *R*-rate position and the ETL, served as electron trapping sites because the transporting electrons had to overcome a barrier of

0.3 eV caused by the LUMO difference between the ADN and the rubrene, thus making the 5 nm layer an electron trapping region. From the hole-transporting point of view, the codoped layer of 10 nm near the HTL in device 11, which worked similarly to that in device 10, did not introduce additional energy barrier for the holes. It should be noted that any effects caused by the electrons were largely excluded in the 10 nm region. Electrons in the 10 nm codoped layer to the left of maximum *R*-rate position were strongly suppressed in favor of holes because less electrons would be left after passing the maximum *R*-rate position due to opposite carrier recombination.

Compared with corresponding control devices, the 3% DPAVBi-doped device 10 achieved a 21.7% reduction, much higher than the 12% in the case of the 2% DPAVBi. According to the earlier report,[19] voltage reduction could be canceled by accumulated carriers. Therefore, the further away from the interface where carrier accumulated the codoped layer covering the maximum *R*-rate position, the lower the device driving voltage.

Focusing solely on the electrical characteristics of device 10, one can see that it exhibited the lowest driving voltage of 7.2 V at 100 mA/cm^2, 112 nits driven at 4 V and 1150 nits at 5.5 V. In terms of emission performance, it demonstrated the highest efficiency of 7.7 cd/A, i.e., 6.2 lm/W at 112 cd/m^2. Within the practical illumination range, the CIE coordinates deviated from (0.34, 0.354) at 112 cd/m^2 to (0.322, 0.337) at 1150 cd/m^2.

D. Comparison with heterojunction white OLED

The structure containing two or three different EMLs is common in the field of white OLED,[3–5] since EMLs emitting complementary color are intuitively stacked to generate white light. In order to elaborate the role of the codoped layer in carrier transport, a white OLED with conventional heterojunction EML structure,[22] for example, rubrene:ADN/DPAVBi:ADN, was fabricated and labeled as device 12, as shown in Fig. 5. This discrepancy between device 5 and 12 accounted for the importance of DPAVBi in the codoped layer. As can be seen from Table I, the heterojunction device 12 pushed its driving voltage backward as compared with reference device 1. It is clear that the energy barrier of 0.4 eV, from rubrene to ADN, essentially created a hole-trap site in the rubrene, from the widely known fact that an energy barrier larger than 0.3 eV presents an efficient barrier to carrier transport.[26]

In device 5, the 2% DPAVBi facilitated the current flow and lowered the driving voltage by 1.1 V, relative to device 12. On top of the multiplication of recombination current, two other intrinsic properties came into play. One was the hole-transporting characteristic of the DPAVBi, while the other was that the HOMO of DPAVBi (5.51 eV) was close to that of rubrene (5.4 eV). During the incorporation of the DPAVBi, more holes could easily be injected from the NPB to the EML and transported through the DPAVBi and ADN. Likewise, holes trapped on rubrene were more likely to hop onto the DPAVBi due to the small energy barrier of 0.1 eV, as illustrated in Fig. 1(b). Following their escape, the holes hopped through the DPAVBi molecules. This two-step process can be referred to as a detrapping effect caused by the DPAVBi.

TABLE II. CIE coordinates of device 5 and 12 at comparable luminance levels. In device 5 (Δx, Δy) from 100 to 2000 nits is (−0.04, −0.036); (Δx, Δy) from 2000 to 8000 nits is (−0.012, −0.013). In device 12 (Δx, Δy) from 100 to 2000 nits is (−0.057, −0.046); (Δx, Δy) from 2000 to 8000 nits is (−0.02, −0.022).

Luminance	100 cd/m^2	2000 cd/m^2	8000 cd/m^2
Device 5	(0.331, 0.338)	(0.291, 0.302)	(0.279, 0.289)
Device 12	(0.373, 0.380)	(0.316, 0.334)	(0.296, 0.312)

Another drawback associated with device 12 was the inefficient utilization of excitons in the EML. At the same level of injection current, the emission from device 12 is more yellowish than that from device 5, not shown here. As evident from the electrical characteristic, a greater prominence of the color yellow in the spectrum indicated that the stronger hole-trapping ability of the EML in device 12 hindered the return of the trapped holes to the ADN matrix. At low current injection, since some excitons were formed and radiatively released on the rubrene through the carrier trapping mechanism, the chromaticity coordinates lied in the proximity of the yellow region. At high current injection, in light of the fully charge-occupied rubrene molecules, additional excitons could only be formed on the DPAVBi molecules, thus shifting the CIE coordinates from the yellow to the bluish-white region. According to Table II, over the same luminescence level from 100 to 8000 cd/m^2, the change in CIE coordinates in device 12 was (−0.077, −0.068), which was larger than that of (−0.052, −0.049) in device 5. The superior color stability in device 5 implies that the codoped method can be used to balance the number of excitons released through the DPAVBi and the rubrene.

In addition, such trapping process not only reduces the electrical current, but also decreases the efficiency. Device 12 attained a maximum efficiency of 4.4 cd/A, which was lower than device 5. Given the same concentration of radiative excitons, the more yellowish emission is expected to be more sensitive to the human eyes, resulting in higher luminance efficiency. However, device 12 failed to live up to this expectation due to the possibly stronger exciton-exciton or exciton-polaron annihilation. Therefore, the architecture of selectively codoped layer can distribute the excitons evenly over the EML to avert the occurrence of exciton quenching.

IV. CONCLUSION

Selectively yellow rubrene-codoped layer had been demonstrated as an efficient method to lower the driving voltage by 2 V without altering the backbone of blue OLED; meanwhile, it also generated white light with CIE coordinates of around (0.33, 0.33) through the mixing of two complementary colors. The codoped technique in this paper, which increases the recombination current, is totally different from the addition of electrically conducting layers, which helps to conduct more carriers in devices. Without the engineering of carrier injection and transport, 112 cd/m^2 was attained at a

relatively low driving voltage of 4 V. This method also eliminates commonly known carrier trapping that often occurs when doping materials into the EML. As a result, a maximum efficiency of 7.7 cd/A and 6.2 lm/W at practical luminous level, 112 cd/m^2, was achieved.

ACKNOWLEDGMENTS

This work was supported by Chi Mei EL Corporation and the National Science Council of Taiwan under Grant NSC 95-2221-E-002-305 and NSC 96-2221-E002-126.

[1]C. W. Tang and S. A. VanSlyke, Appl. Phys. Lett. **51**, 913 (1987).
[2]B. W. D'Andrade and S. R. Forrest, Adv. Mater. **16**, 1585 (2004).
[3]J. Kido, M. Kimura, and K. Nagai, Science **267**, 1332 (1995).
[4]S.-J. Yeh, H.-Y. Chen, M.-F. Wu, L.-H. Chan, C.-L. Chiang, H.-C. Yeh, C.-T. Chen, and J.-H. Lee, Org. Electron. **7**, 137 (2006).
[5]G. Cheng, Y. Zhao, Y. Zhang, S. Liu, F. He, H. Zhang, and Y. Ma, Appl. Phys. Lett. **84**, 4457 (2004).
[6]M. Mazzeo, D. Pisignano, F. Della Sala, J. Thompson, R. I. R. Blyth, G. Gigli, R. Cingolani, G. Sotgiu, and G. Barbarella, Appl. Phys. Lett. **82**, 334 (2003).
[7]Q.-X. Tong, S.-L. Lai, M.-Y. Chan, J.-X. Tang, H.-L. Kwong, C.-S. Lee, and S.-T. Lee, Appl. Phys. Lett. **91**, 023503 (2007).
[8]C. C. Chang, J. F. Chen, S. W. Hwang, and C. H. Chen, Appl. Phys. Lett. **87**, 253501 (2005).
[9]Y. Sun, N. C. Giebink, H. Kanno, B. Ma, M. E. Thompson, and S. R. Forrest, Nature (London) **440**, 908 (2006).
[10]M. A. Baldo, D. F. O'Brien, Y. You, A. Shoustikov, S. Sibley, M. E. Thompson, and S. R. Forrest, Nature (London) **395**, 151 (1998).
[11]G. Cheng, F. Li, Y. Duan, J. Feng, S. Liu, S. Qiu, D. Lin, Y. Ma, and S. T. Lee, Appl. Phys. Lett. **82**, 4224 (2003).
[12]M. A. Baldo, C. Adachi, and S. R. Forrest, Phys. Rev. B **62**, 10967 (2000).
[13]J. H. Lee, Y. H. Ho, T. C. Lin, and C. F. Wu, J. Electrochem. Soc. **154**, J226 (2007).
[14]Y.-S. Wu, S.-W. Hwang, H.-H. Chen, M.-T. Lee, W.-J. Shen, and C. H. Chen, Thin Solid Films **488**, 265 (2005).
[15]C. W. Tang, S. A. VanSlyke, and C. H. Chen, J. Appl. Phys. **65**, 3610 (1989).
[16]V. E. Choong, S. Shi, J. Curless, C. L. Shieh, H.-C. Lee, F. So, J. Shen, and J. Yang, Appl. Phys. Lett. **75**, 172 (1999).
[17]S. W. Culligan, A. C.-A. Chen, J. U. Wallace, K. P. Klubek, C. W. Tang, and S. H. Chen, Adv. Funct. Mater. **16**, 1481 (2006).
[18]H. Aziz, Z. D. Popovic, and N.-X. Hu, Appl. Phys. Lett. **81**, 370 (2002).
[19]C. H. Hsiao, J. H. Lee, and C. A. Tseng, Chem. Phys. Lett. **427**, 305 (2006).
[20]S. C. Tse, S. K. So, M. Y. Yeung, C. F. Lo, S. W. Wen, and C. H. Chen, Chem. Phys. Lett. **422**, 354 (2006).
[21]T. H. Liu, Y. S. Wu, M. T. Lee, H. H. Chen, C. H. Liao, and C. H. Chen, Appl. Phys. Lett. **85**, 4304 (2004).
[22]J. H. Jou, Y. S. Chiu, R. Y. Wang, H. C. Hu, C. P. Wang, and H. W. Lin, Org. Electron. **7**, 8 (2006).
[23]G. He, O. Schneider, D. Qin, X. Zhou, M. Pfeiffer, and K. Leo, J. Appl. Phys. **95**, 5773 (2004).
[24]J. Kalinowski, H. Murata, L. C. Picciolo, and Z. H. Kafafi, J. Phys. D **34**, 3130 (2001).
[25]J. Kalinowski, L. C. Picciolo, H. Murata, and Z. H. Kafafi, J. Appl. Phys. **89**, 1866 (2001).
[26]S. J. Martin, A. B. Walker, A. J. Campbell, and D. D. C. Bradley, J. Appl. Phys. **98**, 063709 (2005).